Self-compressed, spectral broadening of a Yb:YAG thin-disk amplifier

Theresa Buberl,[1] Ayman Alismail,[2,3] Haochuan Wang,[2,4] Nicholas Karpowicz,[4] and Hanieh Fattahi[2,4,*]

[1]*Techincal University of Munich, James-Franc- Str. 1, D-85748 Garching, Germany*
[2]*Department für Physik, Ludwig-Maximilians-Universität München, Am Coulombwall 1, D-85748 Garching, Germany*
[3]*Physics and Astronomy Department, King Saud University, Riyadh 11451, Saudi Arabia*
[4]*Max-Planck Institut für Quantenoptik, Hans-Kopfermann-Str. 1, D-85748 Garching, Germany*

hanieh.fattahi@mpq.mpg.de

Abstract: We demonstrate pulse shortening of 1-ps Yb:YAG thin-disk regenerative amplifier to 500 fs by cross-polarized wave generation (XPW) in a 6 mm BaF_2 crystal. The process is self-compressed and has 8.5% conversion efficiency corresponding to 18 μJ energy. Our theoretical and experimental investigation shows that the factor of $\sqrt{3}$ spectral broadening and pulse shortening in ps-XPW-generation only happens in unsaturated regime. We demonstrate that the initial spectral chirp affects the spectral broadening and pulse shortening of XPW pulses.

OCIS codes: (140.3615) Lasers, ytterbium; (190.4223) Nonlinear-wave mixing; (320.7110) Ultrafast nonlinear optics; (190.4380) Nonlinear optics, four-wave mixing.

References and links

1. H. Fattahi, H. G. Barros, M. Gorjan, T. Nubbemeyer, B. Alsaif, C. Y. Teisset, M. Schultze, S. Prinz, M. Haefner, M. Ueffing, A. Alismail, L. Vámos, A. Schwarz, O. Pronin, J. Brons, X. T. Geng, G. Arisholm, M. Ciappina, V. S. Yakovlev, D.-E. Kim, A. M. Azzeer, N. Karpowicz, D. Sutter, Z. Major, T. Metzger, and F. Krausz, "Third-generation femtosecond technology," Optica **1**, 45–63 (2014).
2. R. Fleischhaker, R. Gebs, A. Budnicki, M. Wolf, J. Kleinbauer, and D. H. Sutter, "Compact gigawatt-class sub-picosecond Yb:YAG thin-disk regenerative chirped-pulse amplifier with high average power at up to 800 kHz," in 2013 Conference on Lasers & Electro-Optics Europe & International Quantum Electronics Conference CLEO EUROPE/IQEC (2013), pp. 1–1.
3. F. Röser, T. Eidam, J. Rothhardt, O. Schmidt, D. N. Schimpf, J. Limpert, and A. Tünnermann, "Millijoule pulse energy high repetition rate femtosecond fiber chirped-pulse amplification system," Opt. Lett. **32**, 3495–3497 (2007).
4. P. Russbueldt, T. Mans, G. Rotarius, J. Weitenberg, H. D. Hoffmann, and R. Poprawe, "400W Yb:YAG Innoslab fs-Amplifier," Opt. Express **17**, 12230–12245 (2009).
5. C. Teisset, M. Schultze, R. Bessing, M. Haefner, S. Prinz, D. Sutter, and T. Metzger, "300 W picosecond thin-disk regenerative amplifier at 10 kHz repetition rate,"in Advanced Solid-State Lasers Congress Postdeadline (2013), paper JTh5A.1.
6. L. E. Zapata, H. Lin, A.-L. Calendron, H. Cankaya, M. Hemmer, F. Reichert, W. R. Huang, E. Granados, K.-H. Hong, and F. X. Kärtner, "Cryogenic Yb:YAG composite-thin-disk for high energy and average power amplifiers," Opt. Lett. **40**, 2610–2613 (2015).
7. C. J. Saraceno, F. Emaury, C. Schriber, M. Hoffmann, M. Golling, T. Südmeyer, and U. Keller, "Ultrafast thin-disk laser with 80 μJ pulse energy and 242 W of average power," Opt. Lett. **39**, 9–12 (2014).
8. O. Pronin, J. Brons, C. Grasse, V. Pervak, G. Boehm, M.-C. Amann, V. L. Kalashnikov, A. Apolonski, and F. Krausz, "High-power 200 fs Kerr-lens mode-locked Yb:YAG thin-disk oscillator," Opt. Lett. **36**, 4746–4748 (2011).

#259464 Received 15 Feb 2016; revised 31 Mar 2016; accepted 31 Mar 2016; published 3 May 2016

9. N. Ishii, L. Turi, V. S. Yakovlev, T. Fuji, F. Krausz, A. Baltuska, R. Butkus, G. Veitas, V. Smilgevicius, R. Danielius, and A. Piskarskas, "Multimillijoule chirped parametric amplification of few-cycle pulses," Opt. Lett. **30**, 567–569 (2005).
10. M. Bradler, P. Baum, and E. Riedle, "Femtosecond continuum generation in bulk laser host materials with sub-μJ pump pulses," Appl. Phys. B **97**, 561–574 (2009).
11. D. Brida, C. Manzoni, G. Cirmi, M. Marangoni, S. Bonora, P. Villoresi, S. De Silvestri, and G. Cerullo, "Few-optical-cycle pulses tunable from the visible to the mid-infrared by optical parametric amplifiers," J. Opt. **12**, 013001 (2010).
12. O. Pronin, M. Seidel, F. Lücking, J. Brons, E. Fedulova, M. Trubetskov, V. Pervak, A. Apolonski, T. Udem, and F. Krausz, "High-power multi-megahertz source of waveform-stabilized few-cycle light," Nat. Commun. **6**, 1–6 (2015).
13. A. Schwarz, M. Ueffing, Y. Deng, X. Gu, H. Fattahi, T. Metzger, M. Ossiander, F. Krausz, and R. Kienberger, "Active stabilization for optically synchronized optical parametric chirped pulse amplification," Opt. Express **20**, 5557–5565 (2012).
14. H. Fattahi, C. Teisset, O. Pronin, A. Sugita, R. Graf, V. Pervak, X. Gu, T. Metzger, Z. Major, F. Krausz, and A. Apolonski, "Pump-seed synchronization for MHz repetition rate, high-power optical parametric chirped pulse amplification," Opt. Express **20**, 9833–9840 (2012).
15. T. Metzger, "High-repetition-rate picosecond pump laser based on a Yb:YAG disk amplifier for optical parametric amplification," PhD thesis, Berlin Tech. University (2009).
16. O. H. Heckl, C. J. Saraceno, C. R. E. Baer, T. Südmeyer, Y. Y. Wang, Y. Cheng, F. Benabid, and U. Keller, "Temporal pulse compression in a xenon-filled Kagome-type hollow-core photonic crystal fiber at high average power," Opt. Express **19**, 19142–19149 (2011).
17. L. Lötscher and L. Vámos, "Long-term stability of nonlinear pulse compression using solid-core large-mode-area fibers," J. Lasers Opt. Photon. **02**, 1–5 (2015).
18. N. Minkovski, G. I. Petrov, S. M. Saltiel, O. Albert, and J. Etchepare, "Nonlinear polarization rotation and orthogonal polarization generation experienced in a single-beam configuration," J. Opt. Soc. Am. B **21**, 1659–1664 (2004).
19. A. Jullien, O. Albert, F. Burgy, G. Hamoniaux, J.-P. Rousseau, J.-P. Chambaret, F. Augé-Rochereau, G. Chériaux, J. Etchepare, N. Minkovski, and S. M. Saltiel, "10^-10 temporal contrast for femtosecond ultraintense lasers by cross-polarized wave generation," Opt. Lett. **30**, 920–922 (2005).
20. M. Lenzner, J. Krüger, S. Sartania, Z. Cheng, C. Spielmann, G. Mourou, W. Kautek, and F. Krausz, "Femtosecond optical breakdown in dielectrics," Phys. Rev. Lett. **80**, 4076–4079 (1998).
21. A. Jullien, L. Canova, O. Albert, D. Boschetto, L. Antonucci, Y.-H. Cha, J. Rousseau, P. Chaudet, G. Chériaux, J. Etchepare, S. Kourtev, N. Minkovski, and S. Saltiel, "Spectral broadening and pulse duration reduction during cross-polarized wave generation: influence of the quadratic spectral phase," Appl. Phys. B **87**, 595–601 (2007).
22. A. Cotel, A. Jullien, N. Forget, O. Albert, G. Chériaux, and C. Le Blanc, "Nonlinear temporal pulse cleaning of a 1-μm optical parametric chirped-pulse amplification system," Appl. Phys. B **83**, 7–10 (2006).
23. A. Ricci, F. Silva, A. Jullien, S. L. Cousin, D. R. Austin, J. Biegert, and R. Lopez-Martens, "Generation of high-fidelity few-cycle pulses at 2.1 μm via cross-polarized wave generation," Opt. Express **21**, 9711–9721 (2013).
24. L. Canova, O. Albert, N. Forget, B. Mercier, S. Kourtev, N. Minkovski, S. M. Saltiel, and R. LopezMartens, "Influence of spectral phase on cross-polarized wave generation with short femtosecond pulses," Appl. Phys. B **93**, 443–453 (2008).
25. T. R. Taha and M. I. Ablowitz, "Analytical and numerical aspects of certain nonlinear evolution equations. II. Numerical, nonlinear Schrödinger equation," J. Comput. Phys. **55**, 203–230 (1984).
26. A. Jullien, C. G. Durfee, A. Trisorio, L. Canova, J.-P. Rousseau, B. Mercier, L. Antonucci, G. Chériaux, O. Albert, and R. Lopez-Martens, "Nonlinear spectral cleaning of few-cycle pulses via cross-polarized wave (XPW) generation," Appl. Phys. B **96**, 293–299 (2009).
27. L. Canova, S. Kourtev, N. Minkovski, A. Jullien, R. Lopez-Martens, O. Albert, and S. M. Saltiel, "Efficient generation of cross-polarized femtosecond pulses in cubic crystals with holographic cut orientation," Appl. Phys. Lett. **92**, 231102 (2008).
28. H. Fattahi, A. Alismail, H. Wang, J. Brons, O. Pronin, T. Buberl, L. Vámos, G. Arisholm, A. M. Azzeer, and F. Krausz, "High-power, 1-ps, all-Yb:YAG thin-disk regenerative amplifier," Opt. Lett. **41**, 1126–1129 (2016).
29. D. T. Morelli and J. Heremans, "Thermal conductivity of single-crystal barium fluoride," J. Appl. Phys. **63**, 573 (1988).
30. M. Schulz, R. Riedel, A. Willner, T. Mans, C. Schnitzler, P. Russbueldt, J. Dolkemeyer, E. Seise, T. Gottschall, S. Hädrich, S. Duesterer, H. Schlarb, J. Feldhaus, J. Limpert, B. Faatz, A. Tünnermann, J. Rossbach, M. Drescher, and F. Tavella, "Yb:YAG Innoslab amplifier: efficient high repetition rate subpicosecond pumping system for optical parametric chirped pulse amplification," Opt. Lett. **36**, 2456–2458 (2011).
31. M. Puppin, Y. Deng, O. Prochnow, J. Ahrens, T. Binhammer, U. Morgner, M. Krenz, M. Wolf, and R. Ernstorfer, "500 kHz OPCPA delivering tunable sub-20 fs pulses with 15 W average power based on an all-ytterbium laser," Opt. Express **23**, 1491–1497 (2015).
32. A.-L. Calendron, H. Çankaya, G. Cirmi, and F. X. Kärtner, "White-light generation with sub-ps pulses," Opt.

#259464 Received 15 Feb 2016; revised 31 Mar 2016; accepted 31 Mar 2016; published 3 May 2016

1. Introduction

Lasers based on Yb-doped materials are spreading in the laboratories around the world due to their cost-effectiveness, robust and turn-key performance, scalability in power and energy, and their emission wavelength near 1 μm. With the central wavelength longer than Ti:Sa laser technology, Yb-doped lasers hold promise to overtake the performance of Ti:Sa lasers in several fields such as spectroscopy, high-field physics and attosecond science. However, Yb:YAG lasers contrary to Ti:Sa lasers, support longer pulse durations: few-ps in high-energy regenerative amplifiers [1–6] and several-hundreds of fs in oscillators [7, 8].

This aspect becomes crucial, when considering them as a pump source for optical parametric chirped pulse amplifiers. Here a major requirement for developing few-cycle OPCPA systems based on Yb:YAG amplifiers, is the availability of broadband seed pulses. Heretofore, this barrier was tackled by using a low-energy broadband spectrum from a Ti:Sa oscillator [9] or additional spectral broadening of a Ti:Sa amplifier in a hollow-core-fiber or bulk [10, 11]. These concepts can be followed in Yb:YAG-pumped-OPCPAs by using a Ti:Sa oscillator to seed the amplifier and OPCPA chain simultaneously [1] , or by using a Yb:YAG oscillator as the front end with an additional spectral broadening stage [12]. However the complexity of the system will be greatly reduced if the broadband seed of OPCPA can be directly generated from the OPCPA pump source [13, 14].

Spectral broadening of ps-pulses based on self-phase-modulation (SPM) in hollow-core-fiber is shown to be unstable [15] and in kagome type hollow-core-fibers [16] or large-mode-area waveguides [17] the input pulse energy is limited to 1 μJ. These systems are complex and alignment sensitive, and moreover, the polarization of broadened pulses degrades in the second case. Alternatively, filamentation in bulk, is not a straightforward and possible approach for ps-pulses as the material damage threshold and critical peak power for ps-driven continuum generation in bulk are of the same order of magnitude. Therefore direct, broadband seed generation from ps-Yb-doped lasers will greatly benefit from a simple approach, which is scalable in terms of input energy, to shorten ps-pulses down to hundreds of fs.

Cross-polarized wave (XPW) generation [18] is a degenerate four-wave mixing process, where the interaction of intense, linearly polarized light with a nonlinear medium results in the generation of a pulse with orthogonal polarization with respect to the input pulse. The nonlinear medium has to have an anisotropic third-order nonlinearity and typically an isotropic linear index. Due to the temporal intensity filtering of the input pulse, the temporal contrast of the XPW pulse is enhanced, its spectral intensity becomes smoother and the spectral bandwidth increases [19]. Unlike SPM, the generated XPW signal can be shorter than the input pulse. For few-fs input pulses, the conversion efficiency and spectral broadening of the XPW pulse is greatly affected by the material's dispersion. Dispersion chirps the input pulse and results in a narrower XPW spectral bandwidth. Therefore, the crystal must be thin, which limits the conversion efficiency.

For input pulses of several-hundreds of fs- or ps-duration, material dispersion does not play a critical role and thicker crystals can be used. Nevertheless the lower damage threshold intensity of material for longer pulses [20] limits the conversion efficiency. So far XPW is mostly used as a technique for increasing the temporal contrast of ultrashort pulses and its great potential as an self-compressed pulse-shortening technique, is overlooked.

In this paper, we address this aspect of XPW for ps-long pulses. We perform a full theoretical and experimental investigation on XPW generation from depleted and undepleted 1-ps pulses. In addition we demonstrate that the pulse-duration of the XPW pulse is influenced by the initial spectral chirp of the input pulse for pulses with several-hundred fs duration [21].

#259464 Received 15 Feb 2016; revised 31 Mar 2016; accepted 31 Mar 2016; published 3 May 2016

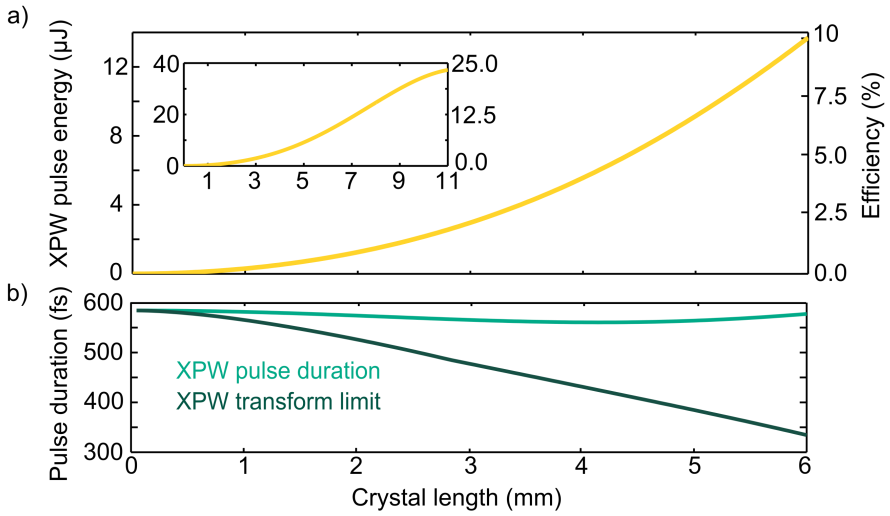

Fig. 1. (a) Simulated conversion efficiency and energy of the XPW signal versus crystal length for 1-ps input pulses in a 6-mm-thick BaF_2 crystal. Inset: the same parameters shown for an 11-mm-thick crystal. (b) Temporal evolution of the XPW signal and its Fourier transform limit pulse duration versus crystal length.

2. Theory

We chose BaF_2 as the nonlinear medium for XPW generation due to its high $\chi(3)$ anisotropy value which allows for good conversion efficiency. Moreover the isotropic linear optical properties of BaF_2 allow perfect group velocity matching along the propagation axis and a perfect spatial overlap of the cross-polarized waves. The crystal also has a wide transmission range from 200 nm to 11μm [22, 23].

Using the slowly evolving envelope approximation, the following coupled wave equations for XPW can be derived:

$$-i\frac{dA}{d\xi} = \gamma_1 AA^*A + \gamma_2 AA^*B + 2\gamma_2 AA^*B + 2\gamma_3 AB^*B + \gamma_3 BBA^* + \gamma_4 BB^*B, \quad (1)$$

$$-i\frac{dB}{d\xi} = \gamma_5 BB^*B + \gamma_4 BBA^* + 2\gamma_4 ABB^* + 2\gamma_3 ABA^* + \gamma_3 AAB^* + \gamma_2 AA^*A, \quad (2)$$

where A and B are the complex amplitude of the input and XPW signal, respectively. ξ is the propagation direction. γ_1 and γ_5 describe SPM; γ_3 cross-phase modulation (XPM); and γ_2 and γ_4 describe XPW [24].

To study the XPW generation of ps-pulses theoretically, the coupled wave equations are solved using a split-step method [25]. The pulse is propagated in the nonlinear medium in the slowly evolving envelope approximation. We considered cylindrical coordinates with the assumption of radial symmetry. Dispersion and diffraction were taken into account. We assumed an input pulse with a Gaussian spatiotemporal profile, and the pulse duration of 1 ps (FWHM) at 1030 nm. The pulse was propagated in a 6 mm-thick, [011]-cut, BaF_2 at a peak intensity of 400 GW/cm^2, where the $\chi(3)$ is assumed to be $1.59\times10^{-22}\, m^2/V^2$ [26]. The coefficients of the coupled-wave equations were taken from [27].

Conversion efficiency and temporal evolution of XPW versus crystal length are shown in Fig. 1(a) and (b), respectively. It can be seen clearly, up to 1 mm propagation length in the crystal,

#259464 Received 15 Feb 2016; revised 31 Mar 2016; accepted 31 Mar 2016; published 3 May 2016

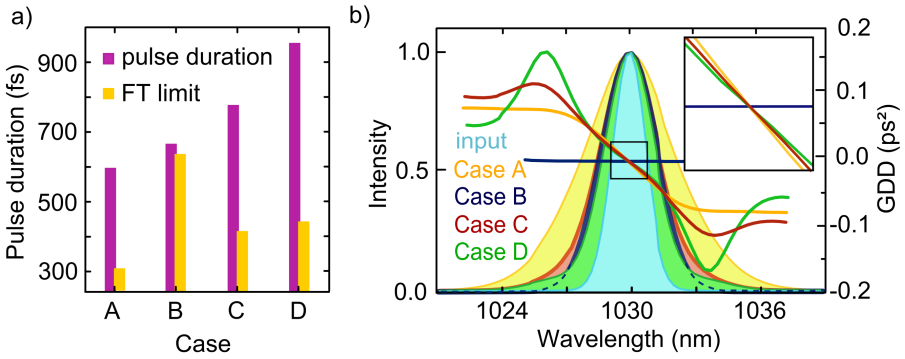

Fig. 2. a) Calculated pulse duration and its Fourier transform limit for different cases explained in the text. b) According spectra and group-delay dispersion after 6 mm propagation.

that the XPW pulse is shorter by a factor of $\sqrt{3}$ compared to the input pulse and stays close to the Fourier transform limit. As the conversion efficiency increases, the duration of the XPW pulse deviates from its temporal Fourier transform limit rapidly, however its Fourier transform limit decreases to support even shorter pulse duration.

At 10% conversion efficiency, the XPW pulse duration is twice its Fourier transform limit. It should be mentioned that the input pulses at this stage are still not depleted. The process reaches saturation in a 11-mm-thick crystal at 23% efficiency (Fig. 1-inset) and supports 173 fs Fourier transform limited pulses. As the dispersion of a 6 mm-thick-BaF_2 on pulses with hundreds of fs is negligible, the observed spectral chirp of the XPW pulses at efficiencies higher that 2% could not be caused by dispersion solely. Therefore we performed a series of simulations to find the origin of the induced phase on the XPW pulse.

To investigate the role of SPM, XPM, and XPW on the spectral phase of the generated pulse with orthogonal polarization, their corresponding coefficients in the coupled wave equation were set to zero, individually. For all cases reported below, the generated cross-polarized pulse has the spectral width of 2.73 nm (FWHM) over the first 3 mm of the crystal. This value corresponds to spectral broadening by a factor of $\sqrt{3}$ for an input spectrum with spectral bandwidth of 1.58 nm. After 3 mm propagation and at the efficiency of 2.5% the spectrum evolves differently. We considered the following cases:

Case A: all third-order nonlinear effects are taken into consideration. In this case the spectrum broadens uniformly by a factor of 2.7, from 1.58 nm (FWHM) to 4.25 nm (FWHM) spectral width after 6 mm propagation in the crystal with 10% conversion efficiency.

Case B: only XPW is considered. Therefore γ_1, γ_3, and γ_5 were set to zero. Here the conversion efficiency decreases to 6.6% and the spectral bandwidth over the crystal thickness stays nearly constant.

Case C: taking into account XPW and SPM results in spectral broadening by a factor of 1.7 to 2.77 nm (FWHM) and conversion efficiency of 5.3%.

Case D: we just considered XPW and XPM in this case which results in spectral broadening by the factor of 1.5 to 2.39 nm (FWHM) and the conversion efficiency of 3.8%.

Comparing spectral broadening and spectral chirp of cases B, C, and D in Fig. 2 shows that the largest spectral broadening and spectral chirp corresponds to case C and D, respectively. By setting γ_1 and γ_5 to zero alternatively, we observed that the SPM of the XPW pulse has the main contribution on spectral broadening and spectral chirp compared to SPM of the input pulse.

Our simulation results indicate that the additional spectral broadening for XPW is caused by

#259464 Received 15 Feb 2016; revised 31 Mar 2016; accepted 31 Mar 2016; published 3 May 2016

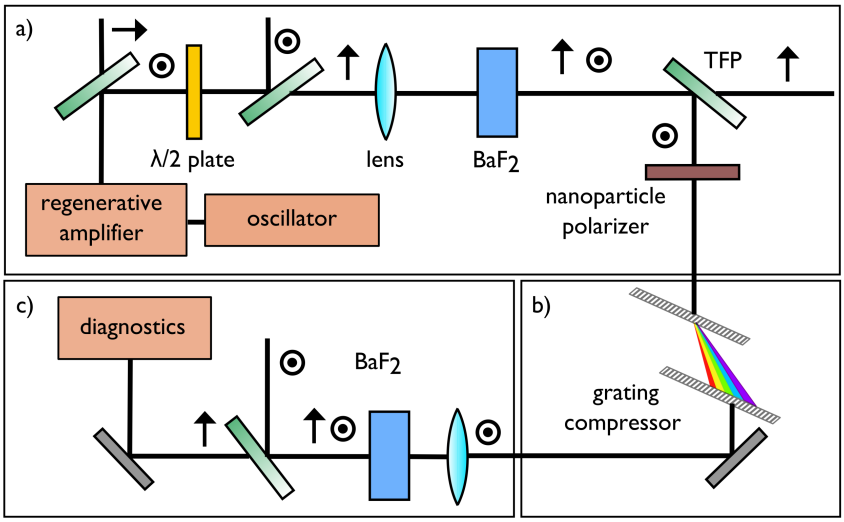

Fig. 3. Linearly polarized input pulses from a Yb:YAG, thin-disk amplifier are focused to a 6-mm-thick BaF_2 to generate cross-polarized waves (XPW). XPW pulses are separated from input pulses using a thin-film polarizer (TFP) and later compressed to their Fourier transform limit in a pair of dielectric gratings. For the case of the cascaded XPW stages, explained in the main text, the XPM beam is focused one more time into a 6 mm BaF_2 crystal. Another TFP is employed to separate the generated from the incident pulse.

interplay of SPM of the XPW pulse and XPM, as at higher efficiencies the peak intensity of the XPW is large enough to initiate these processes. Investigating the spectral phase in each case shows that the introduced group-delay dispersion (GDD) to the generated pulse in case B is zero and the pulse stays Fourier transform limited during its propagation in the crystal. However the other three cases influence the GDD of the pulse in the same manner. Performing simulations without diffraction and dispersion yields the same results.

Therefore we concluded, high efficiency in XPW process comes at the expense of an additional spectral chirp. In the next section we demonstrate the self-compressed pulse shortening of 1-ps pulses in a simple XPW stage. Additionally we show that spectral chirp of the input pulse affects the spectral broadening of the XPW pulses. This is consistent with the theoretical estimation of previous reports [21].

3. Experiment

The experimental setup is shown in Fig. 3. A Yb:YAG thin-disk regenerative amplifier with 20 mJ, 1 ps pulses at 5 kHz repetition rate [28] is used as the front end of the system.

For this study we used 210 μJ of the total energy of the amplifier. The input energy to the XPW setup was adjusted by using an attenuator consisting of a thin-film polarizer (TFP) and a $\lambda/2$-plate. A lens with a focal length of 750 mm was used to focus the beam. A 6-mm-thick BaF_2 crystal with holographic cut, was placed at the focus. As addressed in the introduction, the damage threshold of materials is inversely proportional to the square root of pulse duration [20]. Therefore we performed a study to estimate the damage threshold peak intensity for BaF_2 crystal when irradiated with 1-ps pulses. We observed two damage mechanisms: instantaneous damage, and thermal damage due to nonlinear absorption in the crystal.

When irradiating the crystal at 400 GW/cm^2 peak intensity no immediate damage was ob-

#259464 Received 15 Feb 2016; revised 31 Mar 2016; accepted 31 Mar 2016; published 3 May 2016

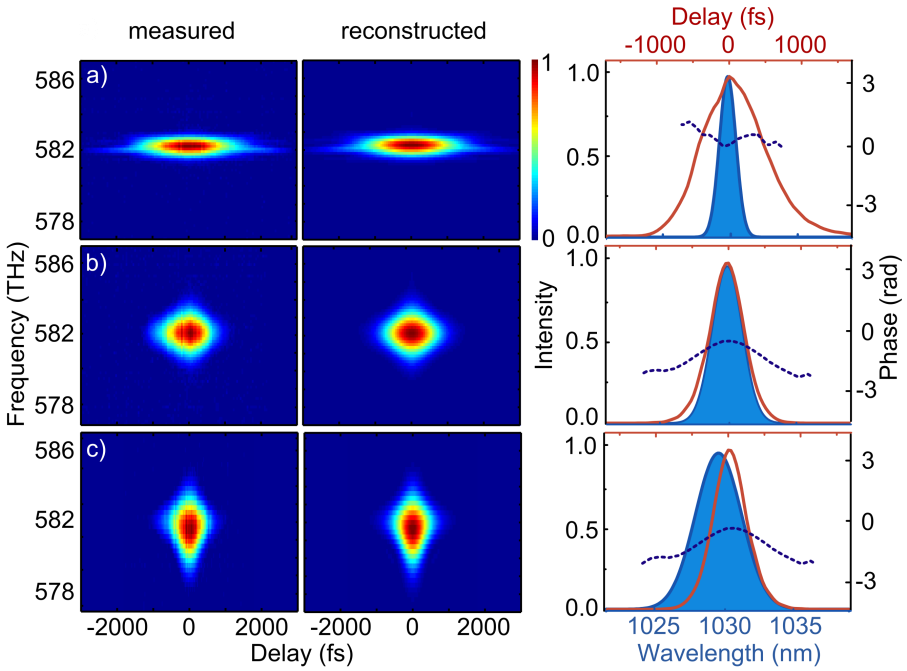

Fig. 4. Input pulse (a) and XPW pulse after each stage (b,c). Left: Measured and retrieved FROG spectrograms. G_{error}: 2.8×10^{-3}, G_{error}: 5.9×10^{-3} and G_{error}: 5.0×10^{-3} respectively. Right: Retrieved time envelopes (red line), intensity spectra (blue line), and spectral phases (blue dashed line).

served. Nevertheless for operation longer than 5 minutes, the crystal was locally damaged. Therefore we chose peak intensity below this value and in addition we placed the BaF_2 crystal approximately 30 mm after the focus. This configuration is beneficial as the divergence of the input beam compensates for the self-focusing of the beam in the BaF_2 crystal. Therefore the peak intensity on the XPW crystal could scale up to 300 GW/cm^2. An anti-reflection coated TFP with $R_P < 2\%$ is used to separate the s-polarized XPW beam from the p-polarized input beam. To enhance the contrast ratio, a nanoparticle linear film polarizer (Thorlabs LPVIS100) is placed after the TFP and aligned to transmit the s-polararized beam. At 210 μJ input energy, 18 μJ XPW signal was generated corresponding to an efficiency of 8.5%.

For temporal characterization of the XPW pulses, a home-built frequency resolved optical gating system based on second harmonic generation (SHG-FROG) containing a 100 μm thick BBO crystal was used. Figure 4(a) and Fig. 4(b) shows the FROG spectrograms and their retrieved counterparts for the input and the XPW pulses, respectively. It can be clearly seen that the XPW pulse is shortened to 537 fs (FWHM) corresponding to the broadening of the spectrum from 1.6 nm to 3 nm. The measured pulse duration is slightly longer than the 398 fs Fourier transform limit of the measured spectrum, indicating the presence of spectral chirp on the XPW pulses. As it was shown in the previous section, the interplay between SPM and XPM leads to additional spectral broadening of the XPW signal and spectral chirp.

We estimated group delay dispersion (GDD) of 6×10^4 fs^2 by calculating the GDD from the retrieved spectral phase of the XPW pulse. A pair of dielectric transmission gratings with a groove density of 1000/mm and 93% throughput in a single-pass configuration was used, which resulted in pulses with 404 fs duration (FWHM).

#259464 Received 15 Feb 2016; revised 31 Mar 2016; accepted 31 Mar 2016; published 3 May 2016

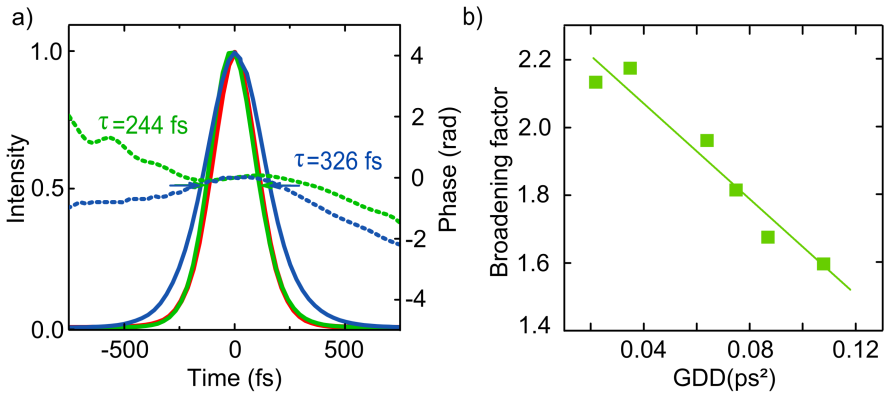

Fig. 5. Second XPW stage: a) Time envelope of the XPW pulse for a chirped (solid blue line) and a compressed (solid green line) input pulse. The dashed lines denote the spectral phase, respectively. The solid red line shows the Fourier transform limit of the XPW pulse for a compressed input pulse. b) Calculated broadening factor for input pulses with increasing group delay dispersion.

As discussed in the previous section, spectral chirp of the input pulse influences the pulse shortening and spectral broadening of the XPW process even for pulses with several hundreds of fs pulse duration. To study the effect of spectral chirp, the generated XPW beam was focused to another 6 mm-thick BaF_2 placed 5 mm behind the focus of a convex lens with the focal length of 100 mm (Fig. 3(c)). Tighter focusing was necessary to reach 150 GW/cm^2 peak intensity on the second crystal as the output of the first stage in our setup was limited to 18 μJ. The beam size on the crystal was 140 μm. Similar to the first stage a TFP was employed to separate the generated and the incident beam.

We deliberately operated the second stage at low conversion efficiency of 3%, corresponding to 500 nJ of energy, to isolate the observed effect of the chirped input pulse from the spectral chirp caused by operating at higher efficiencies.

Figure 4(c) shows the pulse shortening of the second XPW stage to 326 fs without any compression in between the two stages. For input pulses with nearly zero spectral phase the generated XPW at the second stage is 244 fs (FWHM) close to its Fourier transform limit. The XPW pulses in this case, have 25% shorter duration and 18% broader spectral bandwidth (Fig. 5(a)) which is in a good agreement with our simulation.

For detailed study, we measured the spectral phase of the first XPW stage at different conversion efficiencies. Figure 5(b) shows the calculated influence of the measured spectral phases on the XPW pulses at the second stage. It can be clearly seen that operating the first XPW stage at higher conversion efficiencies results in higher spectral phase which reduces the spectral broadening at the second stage.

4. Conclusion and outlook

We report on the generation of 500 fs, 18 μJ pulses, from a 1-ps, Yb:YAG thin-disk regenerative amplifier by employing XPW generation. Our theoretical and experimental study shows that for ps-input pulses at a conversion efficiency of about 3% the generated XPW pulse is self-compressed and shortened by a factor of 1.7. However at higher efficiencies the generated pulse becomes chirped. We showed theoretically that this chirp originates from an interplay between SPM and XPM, enabled by higher XPW intensities at higher conversion efficiency. Additionally our study confirmed that the initial chirp of input pulses longer than hundreds of

#259464 Received 15 Feb 2016; revised 31 Mar 2016; accepted 31 Mar 2016; published 3 May 2016

fs also affects the XPW process and results in less spectral broadening.

In conclusion, we demonstrated XPW as a powerful and simple technique for pulse-shortening of ps-pulses. XPW pulses have excellent temporal contrast, excellent beam profile, and uniform spectrum over the entire spatial profile of the beam. The self-compression of XPW pulses at lower conversion efficiencies eliminates the need for any additional compression stage, while the energy and power scalability of this technique is assured by availability of BaF_2 crystals in large aperture, and its good thermal properties [29], alternatively.

XPW as an initial pulse-shortening step is crucial for direct generation of a stable, octave-spanning spectrum [30–32] from high-energy, 1-ps Yb:YAG amplifiers. The generated broadband spectrum in this way is intrinsically synchronized with the amplifier's pulses and can be used to seed high-energy few-cycle OPCPA chains, eliminating the need for temporal pump-seed synchronization systems [13, 14].

In addition, the unconverted portion of the energy after the XPW stage at low efficiencies maintains its excellent spatiotemporal quality unlike the case of SPM and the other third order processes. This residual energy can be reused to pump the OPCPA stages later, leaving the total efficiency of a system consisting of XPW, the seed generation setup and the OPCPA stages in the same order of the OPCPA's conversion efficiency.

Acknowledgments

We gratefully thank support and discussion with Ferenc Krausz. We acknowledge support from LASERLAB-EUROPE (grant agreement no. 284464, the European Commissions Seventh Framework Programme) and the Munich-Centre for Advanced Photonics.

#259464 Received 15 Feb 2016; revised 31 Mar 2016; accepted 31 Mar 2016; published 3 May 2016